



## Superconductivity of strongly correlated systems / Supraconductivité des systèmes fortement corrélés Oxide interface superconductivity

### Supraconductivité à l'interface d'oxydes

Stefano Gariglio\*, Jean-Marc Triscone

DPMC, University of Geneva, 24 quai E.-Ansermet, CH-1211 Geneva 4, Switzerland

#### ARTICLE INFO

##### Article history:

Available online 19 May 2011

##### Keywords:

Superconductivity  
Complex oxides  
2 dimensionality  
Copper oxides  
Phase diagram  
Electric field effect

##### Mots-clés:

Supraconductivité  
Oxydes complexes  
Bi-dimensionalité  
Cuprates  
Diagramme de phase  
Effet de champ électrique

#### ABSTRACT

This short review covers the emerging research field of interface superconductivity in complex oxide heterostructures. The first part of the paper is devoted to the prediction and observation of an interfacial superconducting state in metallic/insulating copper oxide bilayers. In the second part of the manuscript, the discovery and the modulation of superconductivity at the interface between two insulating oxides,  $\text{LaAlO}_3$  and  $\text{SrTiO}_3$ , is described. These examples serve as an illustration of the potential that interfaces hold for revealing novel electronic behavior in complex oxide heterostructures, opening possibly a path to enhance the critical temperature or to discover new superconductors.

© 2011 Académie des sciences. Published by Elsevier Masson SAS. All rights reserved.

#### RÉSUMÉ

Cette courte revue couvre le champ émergent de recherche de la supraconductivité à l'interface d'oxydes complexes. La première partie est consacrée à la prédiction et à l'observation d'un état supraconducteur à l'interface entre une couche cuprate métallique et une couche cuprate isolante. Dans la deuxième partie du manuscrit, la découverte et la modulation de la supraconductivité à l'interface de deux oxydes isolants, le  $\text{LaAlO}_3$  et le  $\text{SrTiO}_3$ , est décrite. Ces exemples servent à illustrer le potentiel que détiennent les interfaces d'oxydes complexes. Ce champ d'activité pourrait ouvrir la voie à l'augmentation de la température critique ou éventuellement à la découverte de nouveaux supraconducteurs.

© 2011 Académie des sciences. Published by Elsevier Masson SAS. All rights reserved.

## 1. Introduction

100 years after its discovery, the fascination for superconductivity has not dwindled, as illustrated by the numerous events around the 2011 celebration of the discovery of Kamerlingh-Onnes. From the beginning, the ability to drive a current without losses and the observed perfect diamagnetism have aroused widespread amazement. More recently, the sources of continuous appeal have been the different manifestations of this collective quantum state in novel materials and structures. Perhaps the best example is the discovery of high temperature superconductivity in layered copper oxides. In these compounds, superconductivity manifests itself in a rather complex way, with a variety of electronic states occurring at different doping levels. This diversity of behaviors is a remarkable feature of complex oxides in general, in which the carrier concentration often defines the ground state of the system. The different electronic phases (including metallic, insulating

\* Corresponding author.

E-mail addresses: Stefano.Gariglio@unige.ch (S. Gariglio), Jean-Marc.Triscone@unige.ch (J.-M. Triscone).

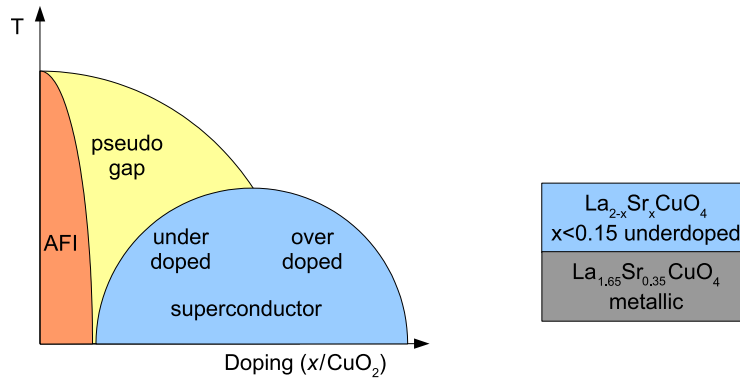


**Fig. 1.** Left: Schematic temperature doping phase diagram of high temperature superconductors. Adding carriers ( $x$ ) to the copper oxide planes turns an antiferromagnetic insulator (AFI) into a superconductor. The optimal critical temperature separates the underdoped and the overdoped regions. Right: Schematic of the heterostructure designed for enhancing  $T_c$  in high temperature superconductors.

and superconducting as well as different magnetic states) can thus be accessed by modulating the doping level of the system. Since correlated oxides display a variety of electronic properties that can be found in compounds that share a similar crystalline structure, these materials can be stacked into artificial heterostructures. Such composite structures become particularly exciting when their electronic properties differ from the ones of the constituents' and from their "weighted average". This approach has been widely used in semiconductor heterostructures, where two-dimensional electron gases with extremely high mobilities have been produced. These efforts lead to new electronic states and amazing phenomena such as integer and fractional quantum Hall effect. In oxides, the number of combinations is enormous, promoting an intense research effort in oxide heterostructures and interface physics [1]. Recent review articles on the exciting field of oxide interface physics can be found in Refs. [2,3].

Among the possible phenomena which can be generated at interfaces, superconductivity is of particular interest. The natural breaking of inversion symmetry at a surface or an interface is known to generate additional electronic states in the band diagram of a system. This breaking of symmetry also promotes a spin-splitting of the bands due to the Rashba-Bychkov effect [4]. Signatures of spin-splitting at surfaces of metallic Pb [5] and in oxide LaAlO<sub>3</sub>/SrTiO<sub>3</sub> heterostructures [6,7] have already been observed, the theoretically predicted effects on their superconducting states [8], however, are yet to be revealed. Another important phenomenon that can occur at an interface is charge transfer which results in a change in the interfacial charge density. In materials where the ground state is determined by the carrier concentration, such as high temperature superconductors, this may have important consequences. For instance, at interfaces between high-temperature superconducting YBa<sub>2</sub>Cu<sub>3</sub>O<sub>7</sub> and magnetic metallic La<sub>0.67</sub>Ca<sub>0.33</sub>MnO<sub>3</sub>, charge transfer seems to be at the origin of an orbital reconstruction on the Cu site [9,10]. This interface effect leads to induced magnetism in the superconductor and to a change in the ferromagnetic domain structure at the superconducting transition temperature [11]. Modifications of the carrier density can be also induced by the electric field-effect. Recently, in SrTiO<sub>3</sub> single crystals [12] and Nb-doped SrTiO<sub>3</sub> thin films [13], remarkable changes of the superconducting properties were obtained upon gate voltage tuning (for a review, refer to [14,15]). In this review, we will focus on recent observations of exciting superconducting phenomena that occur at oxide interfaces. In the first part of the manuscript, we will describe the realization of an interfacial superconducting state with a high critical temperature between metallic and insulating cuprate films. In the second part, we will discuss the discovery and the modulation of superconductivity at the interface between two insulating compounds, LaAlO<sub>3</sub> and SrTiO<sub>3</sub>. We will then briefly compare these two systems and discuss some possible future research directions.

## 2. Interfacial superconductivity in copper oxide structures

The phase diagram of hole-doped high temperature superconductors displays a variety of electronic states that strongly depend on the doping level of the system, as shown schematically in Fig. 1. How these phases influence the superconducting state is still a matter of debate. What seems to be clear is that the physics of the underdoped and overdoped regime is different. A series of works has investigated a route to combine the characteristics of both regimes in artificial structures in order to try enhancing the superconducting critical temperature ( $T_c$ ). In this approach, the starting assumption is that, in the underdoped region, local superconducting pairing persists up to temperatures well above the maximum observed  $T_c$ , giving rise to the pseudogap phase. The factor limiting  $T_c$  (the establishment of phase coherence between the preformed pairs) is thought to be phase fluctuations linked to the low superfluid density and associated small phase stiffness. The idea suggested by Kivelson and coworkers is to design an artificial composite that combines the high pairing energy of the underdoped regime with the large superfluid density, typical of a metal or an overdoped cuprate [16]. According to their calculations, a system consisting of a material with a high pairing energy ( $\Delta_o$ ) but low or zero  $T_c$  and a metallic compound with low pairing energy but large carrier density, may display a  $T_c$  on the scale of  $\Delta_o$  [17]. Such an effect requires an optimal coupling of the two components via the tunneling of electrons across the interface.

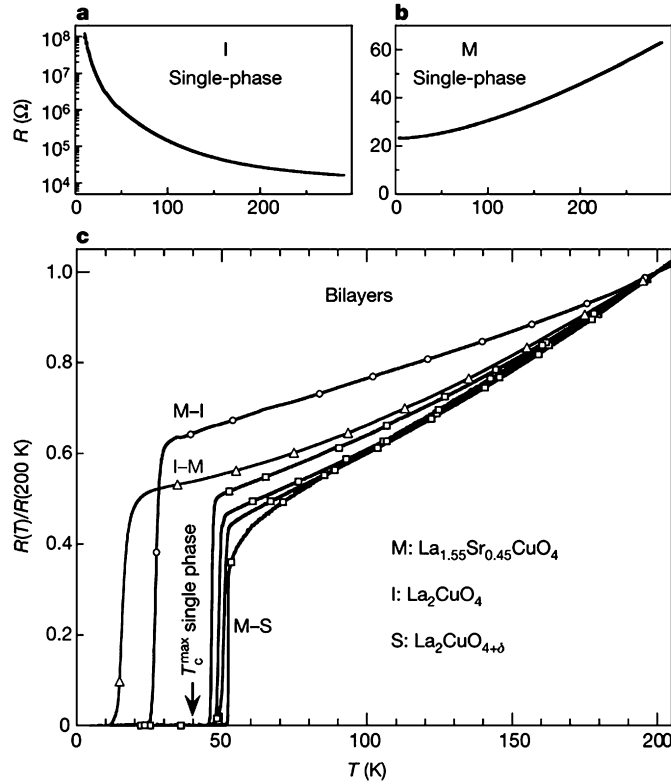


**Fig. 2.** Resistance curves as a function of temperature of single-phase and bilayer copper oxide films. The combination of an insulating (I)  $\text{La}_2\text{CuO}_4$  layer and a metallic (M)  $\text{La}_{1.55}\text{Sr}_{0.45}\text{CuO}_4$  layer, whose resistance versus temperature curves are shown in panels a and b respectively, yields a superconducting bilayer structure (panel c). For bilayers composed of superconducting (S)  $\text{La}_2\text{CuO}_{4+\delta}$  and metallic cuprate, the critical temperature exceeds that of the single phase. Reproduced with permission from [22].

With the enticing prospect of raising  $T_c$  above that of both components, this prediction has been tested in multilayers composed of underdoped and overdoped cuprates. The system of choice has been  $\text{La}_{2-x}\text{Sr}_x\text{CuO}_4$ , where the doping can be changed by controlling precisely the La/Sr ratio of each atomic layer. A systematic study of metallic  $\text{La}_{1.65}\text{Sr}_{0.35}\text{CuO}_4$ -superconducting  $\text{La}_{2-x}\text{Sr}_x\text{CuO}_4$  bilayers (where  $x$  was varied from the underdoped to the overdoped regime) has revealed an enhancement of  $T_c$  for  $x < 0.15$ , i.e. for underdoped layers [18]. The maximum  $T_c$ , achieved for  $x = 0.12$ , is higher than the one of the optimally doped bare film. Magnetization and transport measurements suggest that the enhancement of superconductivity occurs precisely at the interface between the layers. Indeed, analyzes of the transport properties (temperature dependence of the resistance and current-voltage characteristics) across the superconducting transition point to a Berezinskii–Kosterlitz–Thouless behavior, expected for a two-dimensional system [19–21]. No such signatures of a two-dimensional behavior were observed for single films. The authors attribute these results to the combination of the high pairing energy of the underdoped layer with the increased phase stiffness induced by pair-propagation through the overdoped component, as predicted by Kivelson and coworkers. It is worth noticing that no  $T_c$  enhancement was observed when the same underdoped layer ( $x = 0.12$ ) was covered with a gold film, possibly because the differences in the Fermi wave vectors and lattice structures of the two materials could reduce the transparency of the interface and thus the tunneling amplitude across the interface. Importantly, it indicates that screening due to the top metallic layer is not responsible for the enhancement of  $T_c$  observed in bilayers.

In a series of experiments, Bozovic and coworkers studied such cuprate interfaces grown by oxide atomic layer-by-layer molecular beam epitaxy [23]. In bilayers consisting of an insulator (I,  $\text{La}_2\text{CuO}_4$ ) and a metal (M,  $\text{La}_{1.55}\text{Sr}_{0.45}\text{CuO}_4$ ), both layers being not superconducting by themselves, interface superconductivity was observed with a  $T_c$  of up to 30 K [22] (see Fig. 2). To determine the spatial extension of this superconducting interface state, a series of M–I and I–M structures was fabricated. The bottom layer thickness was fixed to 30 unit cells while the top one was increased by half a unit cell at a time. From the resistive transitions, it appears that  $T_c$  reaches its highest value already for a 2 unit cells thick top layer. The confinement of superconductivity to a thin interfacial layer was confirmed by measurements of critical current densities ( $j_c$ ) performed using a two-coil mutual inductance technique. In metal-superconducting bilayers,  $j_c$  versus temperature measurements revealed two linear regimes. The first, starting at  $T_c$ , was attributed to the interface superconducting state and the second, appearing at lower temperature, was related to superconductivity developing in the layers. From the analysis of the current densities, an estimate of the enhanced superconducting layer thickness yielded one unit cell. Is the effect observed an

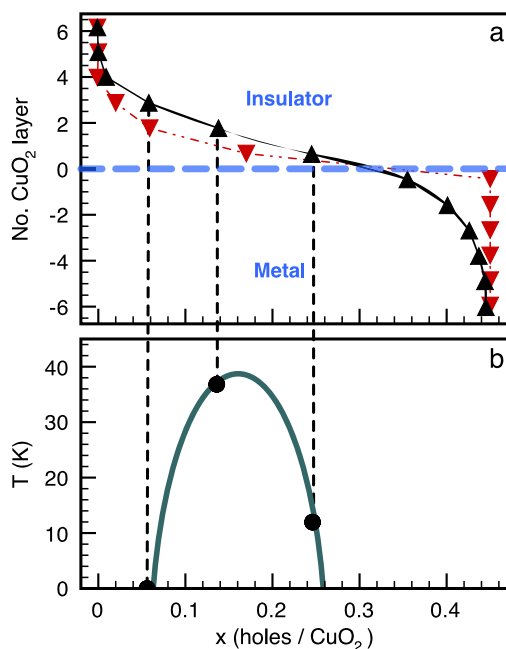


**Fig. 3.** Dopant and charge profile in an insulating-metallic  $\text{La}_2\text{CuO}_4$ - $\text{La}_{1.65}\text{Sr}_{0.35}\text{CuO}_4$  bilayer. (a) The Sr concentration profile (red triangles) measured by local probes was used to calculate the charge profile (black triangles) in the structure. Considering the one-to-one correspondence between the carrier density and the critical temperature (green line in the (b) panel), the charge redistribution for each layer can explain the large  $T_c$  observed. Data from [28].

“intrinsic” interface property or is it due to charge accumulation arising from cation interdiffusion? A series of different local chemically sensitive probes, employed to answer this question, sets an upper limit of less than one unit cell for the cation intermixing.

Further theoretical studies in underdoped-overdoped superlattices using dynamical mean-field techniques reproduced the enhancement of the superconducting order parameter in such structures, with a transition temperature that exceeds the maximum  $T_c$  of single layers [24]. An important observation arising from these calculations is that the hole density profile is the result of charge transfer among the constituent layers. Investigation of the charge distribution in insulating  $\text{La}_2\text{CuO}_4$ /overdoped  $\text{La}_{1.64}\text{Sr}_{0.36}\text{CuO}_4$  superlattices by resonant soft X-ray scattering indicates that the hole distribution varies more gradually than that of the  $\text{Sr}^{2+}$  ions, suggesting a redistribution of holes among the layers [25]. The carriers are not bound to the  $\text{Sr}^{2+}$  dopants but spread over a distance estimated to be  $\sim 6$  Å. This estimate is in agreement with previous observations in  $\text{LaTiO}_3/\text{SrTiO}_3$  heterostructures where the layers were artificially doped by charge redistribution across chemically sharp interfaces [26]. The new arrangement of mobile charges effectively dopes the “insulating” layer, suggesting that superconductivity arises on the “insulating side” of the structure.

To test this idea, Gozar et al. have realized an experiment where the different  $\text{CuO}_2$  planes were selectively doped with Zn atoms, a dopant known to suppress superconductivity. This experiment can thus reveal the precise location of superconductivity [22]. The results reveal a dramatic decrease of the critical temperature when 3% of Cu ions were substituted with Zn within a single atomic plane of the “insulating” layer. This observation and the charge profile calculated from the distribution of the Sr ions shown in Fig. 3 suggest that optimal doping is achieved for the second  $\text{CuO}_2$  plane on the insulating side of the bilayer and hence high temperature superconductivity is located on this particular plane.

These experiments beautifully showed that a single  $\text{CuO}_2$  plane can sustain high-temperature superconductivity. They also highlight the importance of charge transfer for interface superconductivity in metal-insulator structures. The exciting prospect of using heterostructures to enhance the critical temperature certainly deserves further investigations [27].

### 3. Superconductivity at the $\text{LaAlO}_3/\text{SrTiO}_3$ interface

In the quest for artificial charge doping in perovskite superlattices, Ohtomo and Hwang discovered in 2004 that the interface between a  $\text{LaAlO}_3$  (LAO) thin film and a (001)  $\text{SrTiO}_3$  (STO) substrate,  $\text{TiO}_2$  terminated, is conducting, although both materials are wide-bandgap insulators [29]. This report attracted a lot of attention and launched worldwide intense research activities to try understanding the origin of the conduction and also to explore possible novel electronic states in an electron gas confined between two complex oxides.

To obtain a conducting interface, LAO layers with thicknesses larger than 3 unit cells (uc) are typically grown by pulsed laser deposition at  $\sim 800^\circ\text{C}$  in  $\sim 10^{-4}$  mbar  $\text{O}_2$  on  $\text{TiO}_2$ -terminated (001) surfaces of STO single crystals and then cooled to

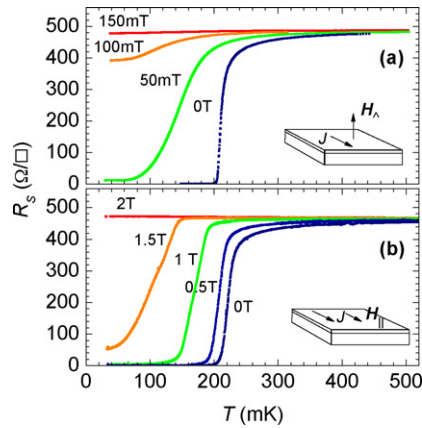


**Fig. 4.** Resistive transitions of a 4 uc LAO/STO sample as a function of temperature  $T$  for magnetic fields applied perpendicular ( $\mu_0 H_{\perp}$ ) and parallel ( $\mu_0 H_{\parallel}$ ) to the interface. Reproduced with permission from [40].

room temperature in a high oxygen pressure. At 4.2 K, the samples exhibit typically a Hall carrier density between 1.5 and  $5 \times 10^{13}/\text{cm}^2$  and mobilities in the range 300–1000  $\text{cm}^2/\text{Vs}$  [30].

Since the discovery of Ohtomo and Hwang, the origin of the charge carriers has been a matter of discussion. Originally, it has been related to the polar nature of the atomic planes of the LAO layer that alternates  $(\text{AlO}_2)^{-1}$  and  $(\text{LaO})^{+1}$ , planes of opposite charge. When grown on a non-polar material like STO, a polar discontinuity is found at the interface [31]. In the absence of external screening, the dipole field inside the layer can be accommodated by polarizing the material through a large polar displacement of the  $\text{La}^{2+}$  and  $\text{O}^{2-}$  ions [32]. However, due to the finite dielectric constant of LAO, this screening is imperfect and, above a critical thickness, it can be energetically more favorable for the layer to screen the remaining field (estimated to be 1 V/uc in the LAO layer [33,34]) by transferring electrons from the O 2p valence band of LAO to the Ti 3d conduction band of STO, forming an electron gas at the interface. This polar catastrophe scenario proposed to explain the conductivity observed in the system has been challenged by the experimental observation of a strong sensitivity to the oxygen pressure during the fabrication of these heterostructures [35] and of ionic intermixing across the interface [31,36,37]. In favor of the electronic reconstruction mechanism proposed in the polar catastrophe scenario, there is the experimental observation of a minimum critical thickness of 4 uc of LAO, necessary to observe a metallic interface [38]. However, the amount of carriers observed does not account for a complete screening of the LAO polarization. This and other discrepancies have kept alive the debate on the origin of the carriers at the interface. In parallel to these studies and as described below, it has been found that this system displays amazing electronic properties which can be linked to the interfacial nature of the electron gas, definitively justifying the attention paid to this fascinating oxide interface.

In 2007, in a collaboration between the teams of Jochen Mannhart and Jean-Marc Triscone, it was discovered that the interface undergoes a transition into a superconducting state when cooled to temperatures below a few hundred mK [39]. The anisotropy and dimensionality of the superconducting state have been assessed by investigating the dependence of the transport properties on the orientation of the applied magnetic field [40]. Fig. 4 shows sheet resistance  $R_S$  vs temperature measurements for magnetic fields applied perpendicular ( $H_{\perp}$ ) and parallel ( $H_{\parallel}$ ) to the interface. In the parallel configuration, the current direction is collinear with the magnetic field. The alignment between the interface and the field is adjusted with a precision of about 0.15 deg using a piezoelectric goniometer.

The analyses of the perpendicular field data lead to an in-plane coherence length  $\xi(0\text{K})$  of about 70 nm. According to the Ginzburg–Landau theory, a superconducting film in the two-dimensional limit (the thickness  $t$  is smaller than the superconducting coherence length) should display a square-root of  $T$  dependence of the parallel critical field. The  $H_{\parallel}(T)$  behavior observed for LAO/STO interfaces is in remarkable agreement with this prediction and allows the superconducting thickness  $t$  to be estimated using the relation  $t = (\sqrt{3}\phi_0)/(\pi\xi(T)\mu_0 H_{\parallel}(T))$ . The data analysis leads to a temperature independent estimate of  $t = 12 \pm 2$  nm. This value, much smaller than the in-plane coherence length, allows the internal consistency of the analysis to be checked.

Having established the dimensionality of the superconducting state, its superconducting transition should bear indications of a Berezinskii–Kosterlitz–Thouless (BKT) transition [19–21]. At the BKT transition temperature, the current-induced Lorentz force causes vortex–antivortex pairs to unbind. In an ideal system, the voltage current characteristics should be of the form  $V \propto I^{a(T)}$  with the  $a$  parameter displaying a jump at  $T_{\text{BKT}}$  from  $a = 1$  for  $T > T_{\text{BKT}}$  to  $a = 3$  at  $T_{\text{BKT}}$ . The  $V(I)$  characteristics, recorded at different temperatures, however do not show evidence of a jump in the  $a$  exponent value but reveal a smooth increase of the  $a$  value. Defining  $T_{\text{BKT}}$  as the temperature at which the  $a$  exponent is equal to 3 yields  $T_{\text{BKT}} = 188$  mK. Further evidence for dissociation of vortices at the superconducting transition can be obtained by examining the resistive transition. Close to the BKT temperature, the correlation length is predicted to diverge with an exponential temperature dependence. The resistance  $R$ , which is proportional to the density of unbound vortices is thus expected to vary with temperature as  $R = R_0 \exp(-b_R/(T - T_{\text{BKT}})^{1/2})$ , where  $b_R$  is a parameter related to the vortex properties [41].

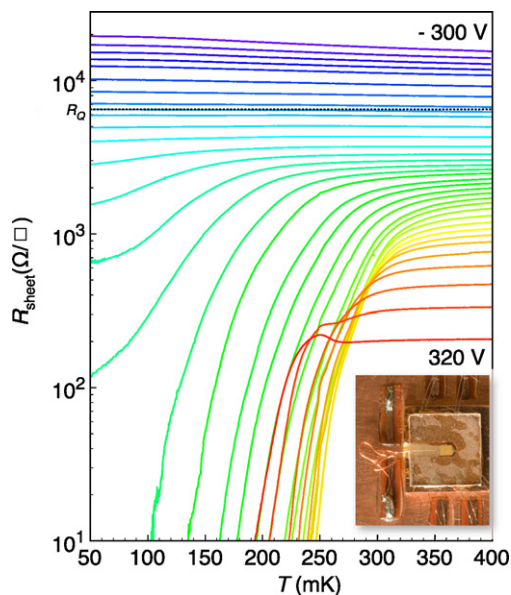


**Fig. 5.** Field-effect experiments on LAO/STO interfaces. Field-effect modulation of the sheet resistance  $R_{\text{sheet}}$  plotted on a semi-logarithmic scale for gate voltages between  $-300$  V and  $320$  V. Inset: a picture of a field-effect device allowing Hall effect and the resistance to be measured. The substrate is a  $5 \times 5$  mm<sup>2</sup> STO crystal. Thin aluminum wires contact the current and voltage pads. The gate voltage is applied between the gold plate on the back of the substrate and the electron gas, which is kept at ground. Data from [45].

Using this relation, an estimate of  $T_{\text{BKT}} \sim 190$  mK is obtained – a value in good agreement with the one extracted from the  $V(I)$  characteristics for the same sample. The analysis discussed above relies on the assumption that the mean field  $T_c$  is far larger than  $T_{\text{BKT}}$ . For this system, the values of the critical currents suggest that the consistency with the BKT scenario requires a high density of vortex–antivortex pairs and the formation of a vortex–antivortex crystal as discussed by Gabay and Kapitulnik [42]. Benfatto and collaborators have questioned this point of view and have proposed an interesting alternative approach [43]. They suggested that the superconducting transition should cross over from a regime of Ginzburg–Landau fluctuations, characterized by a power-law divergence of the correlation length, to a BKT regime where the divergence acquires an exponential form. Accordingly, analyzing the experimental data with a formula interpolating the two regimes, a very good fit is obtained over a wide temperature range with  $T_{\text{BKT}}$  close to  $T_c$ . The behavior of the transport properties at the lowest temperatures deviates from the prediction of both scenarios. In the analysis of Benfatto et al., the resistive tail of the transition could only be fitted by including a Gaussian distribution of the superfluid density. The influence of inhomogeneities and finite size effects may be responsible for the observed behavior. Indeed, as investigated theoretically [44], finite size effects limit the exponential divergence of the coherence length and smooth the BKT transition. This results in  $V(I)$  characteristics displaying a smooth increase of the  $a$  exponent consistent with the data, instead of the predicted jump in  $a(T)$  from 1 to 3 at  $T_{\text{BKT}}$ . More experiments are however necessary to discriminate between the two scenarios.

We now turn to the amazing tunability of the electronic properties at the LAO/STO interface. A very special feature of this system is the fact that the electron gas is naturally sandwiched between two wide bandgap insulators. Additionally, the electron gas displays a low carrier density (typically of the order of  $\sim 10^{13}$  electrons/cm<sup>2</sup>) – one thus realizes that this is the perfect configuration for field-effect experiments. Both insulators can be used as gate dielectric. Most of the experiments to date have used the STO as a (back-)gate dielectric. A typical field-effect device is shown in Fig. 5. In order to modulate the carrier concentration at the interface, an electric field was applied across the 0.5 mm thick STO substrate characterized by a very large dielectric constant at low temperatures [45]. To quantify the change in carrier density resulting from the field-effect, the differential capacitance  $C(V_G) = dQ(V_G)/dV_G$  of the device as a function of the applied gate voltage  $V_G$  has been measured, with  $dQ(V_G)$  being the induced charge for a  $dV_G$  voltage change. Integration of  $C(V_G)$  on the gate voltage sweep allows the total induced charge to be determined. With this approach, the field dependence of the STO permittivity is taken into account [46]. The achievable modulation of the carrier density is remarkably close to the total number of mobile carriers present in the system, indicating that the electric field effect is an excellent tool to probe the phase diagram of the system. The modulation of the conductance upon different gate voltages is shown in Fig. 5. For large negative voltages, corresponding to the smallest accessible electron densities, the sheet resistance increases as the temperature is lowered, suggesting an insulating ground state. Analysis of the variation of the conductance points to a weak localization regime [47]. The loss of phase coherence seems to be related to electron–electron scattering events [41]. The dependence of the sheet resistance in a perpendicular magnetic field confirms this indication: above  $\sim 1$  T the resistance decreases logarithmically with increasing magnetic field, as expected if weak localization is governing the magnetotransport properties.

Increasing further the electric field (and the electron density) drives the system to superconductivity. The transition from the superconducting to the insulating ground state occurs at a critical sheet resistance  $R_c \sim 4.5$  k $\Omega$ , close to the

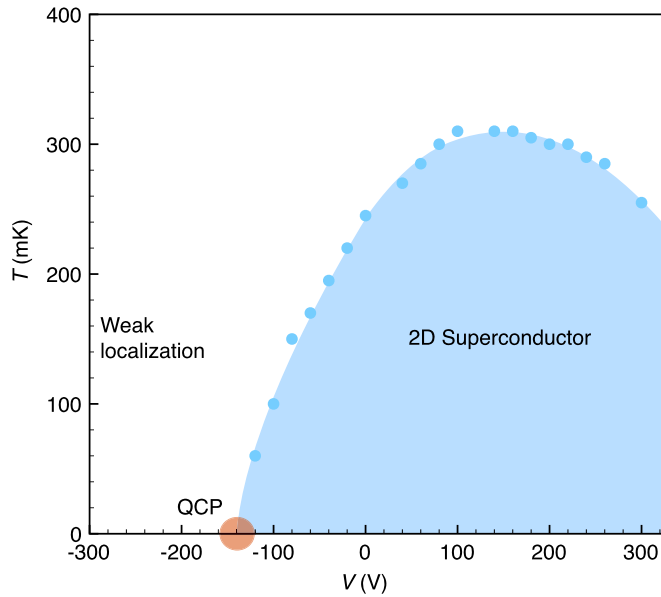


**Fig. 6.** Electronic phase diagram of the LAO/STO interface revealed by the electric field tuning of the carrier density. A quantum critical point (QCP) separates a region characterized by weak-localization from a superconducting groundstate. Data from [45].

quantum of resistance for charge  $2e$  bosons ( $R_q = 6.4$  k $\Omega$ ). Increasing further the carrier density allows a remarkable tuning of the superconducting critical temperature.  $T_c$  progressively increases, reaching a maximum value of 310 mK at optimum doping and then decreases, revealing a superconducting dome shown in Fig. 6, qualitatively similar to that of copper oxides. Further electron doping induces a complete suppression of superconductivity revealing a metallic state at high doping levels [48]. Two quantum critical points thus separate the superconducting phase from an insulating and a metallic state. The modulation of the electronic properties at the LAO/STO interface was originally discussed primarily in terms of changes in the carrier density. More recent work has shown that the mobility also changes dramatically across the phase diagram [48].

A scaling analysis of the quantum critical region [45,41] for the insulating–superconducting phase transition reveals a critical behavior characteristic of a quantum two-dimensional XY system [49]. The loss of the zero resistance superconducting state may thus not be related to an increase of disorder but to the loss of phase coherence due to quantum fluctuations in a clean two-dimensional system, an observation consistent with the observed weak-localization-induced insulating phase.

An important element concurring to the insulator–superconductor transition was revealed by analyzing the magnetoresistance behavior for different doping values across the quantum critical point [6]. Indeed, a remarkable coupling between spin dynamics and transport is apparent in the magnetoconductance measured at 1.5 K, well above the superconducting fluctuation regime. For large negative gate voltages, a large positive magnetoconductance, signature of the weak-localization regime, is measured. As the voltage is increased, a negative magnetoconductance at low field appears. Increasing the gate voltage further, the negative magnetoconductance regime broadens out with the magnetoconductance becoming completely negative up to the largest applied magnetic field (8 T) for the highest electric field. This behavior can be related to the development of a strong spin–orbit coupling, which leads to a weak-antilocalization transport regime. Comparing the evolution of the superconducting  $T_c$  and of the spin–orbit coupling strength reveals a remarkable correlation: the superconducting dome develops as the weak-antilocalization regime appears. This observation suggests that the spin–orbit interaction promotes a two-dimensional delocalized phase which condenses into a superconducting state. The origin of the spin–orbit coupling can be related to the interfacial breaking of structural inversion symmetry. In fact, the analysis of the evolution of the spin relaxation time with the system mobility reveals that the spin–orbit is of the Rashba type demonstrating that the electronic properties measured are linked to the interfacial nature of the system.

The transition from the superconducting to the insulating state can also be driven by a magnetic field. Indeed this control parameter has been widely used to drive superconductor to insulator transitions in thin films such as  $\alpha$ -InO $_x$  [50] and MoGe [51,52]. In this case the hallmark of the transition is the crossing of the magnetoresistance curves recorded at different temperatures at a well defined magnetic field. For carrier densities lower than the optimal doping, a well defined crossing point is observed, revealing a superconductor–insulator transition. In the overdoped regime, no crossing point is observed, which indicates that, on this side of the dome, a superconductor to metal transition occurs. Scaling analysis of these transitions will reveal if their nature is similar or different from the one obtained by electric field tuning.

#### 4. Conclusions and perspectives

In this short review, we have discussed recent experiments demonstrating interfacial superconductivity in two fascinating and rather different systems. While trying to achieve a coupling between order parameters across a bilayer consisting of

an underdoped and an overdoped cuprates, it was discovered that superconductivity can reside in a single  $\text{CuO}_2$  layer and furthermore an enhancement of  $T_c$  above that of the bulk compound is feasible in such copper oxide bilayers. These results were attributed to a chemical profile that confines the optimal electronic doping of the system to a single atomic layer. By contrast, the unexpected appearance of a superconducting 2DEG at the interface between LAO and STO, two band insulators, may be of a purely electronic origin. The high dielectric permittivity of STO, where the electron gas resides, allows an efficient tuning of the metallic and superconducting properties of this unusual 2DEG through field-effect, giving a powerful tool for further studies of 2D superconductivity as well as opening new possibilities for applications. Particularly exciting is the perspective to define conducting and superconducting circuits with nanoscale resolution in this 2DEG. Recent experiments have shown that an electric field applied with the metallic tip of an atomic force microscope can be used to control the conduction of the interface [53]. With this technique, electronic nanostructures and superconducting elements like Josephson junctions and superconducting quantum interference devices (SQUIDs) can potentially be realized. Also, along with the improvement of the mobility, which today is reaching  $\sim 10,000 \text{ cm}^2/\text{Vs}$  [54], mesoscopic physics experiments may be performed on a system whose physical parameters are very different from those observed in III-V semiconductor heterostructures [27], hopefully leading to new devices, functionalities and novel exciting phenomena.

## References

- [1] E. Dagotto, When oxides meet face to face, *Science* 318 (2007) 1076.
- [2] J. Mannhart, D.G. Schlom, Oxide interfaces—an opportunity for electronics, *Science* 327 (2010) 1607–1611.
- [3] P. Zubko, S. Gariglio, M. Gabay, Ph. Ghosez, J.-M. Triscone, Interface physics in complex oxide heterostructures, *Ann. Rev. Cond. Matt. Phys.* 2 (2011) 141–165.
- [4] Y.A. Bychkov, E.I. Rashba, Properties of a 2d electron gas with lifted spectral degeneracy, *JETP Lett.* 39 (1984) 78.
- [5] J. Dil, F. Meier, J. Lobo-Checa, L. Patthey, G. Bihlmayer, J. Osterwalder, Rashba-type spin-orbit splitting of quantum well states in ultrathin Pb films, *Phys. Rev. Lett.* 101 (2008) 266802.
- [6] A.D. Caviglia, M. Gabay, S. Gariglio, N. Reyren, C. Cancellieri, J.-M. Triscone, Tunable Rashba spin-orbit interaction at oxide interfaces, *Phys. Rev. Lett.* 104 (2010) 126803.
- [7] M. Ben Shalom, M. Sachs, D. Rakhmievitch, A. Palevski, Y. Dagan, Tuning spin-orbit coupling and superconductivity at the  $\text{SrTiO}_3/\text{LaAlO}_3$  interface: A magnetotransport study, *Phys. Rev. Lett.* 104 (2010) 126802.
- [8] E. Cappelluti, C. Grimaldi, F. Marsiglio, Topological change of the Fermi surface in low-density Rashba gases: Application to superconductivity, *Phys. Rev. Lett.* 98 (2007) 167002.
- [9] J. Chakhalian, J.W. Freeland, G. Srajer, J. Stremper, G. Khaliullin, J.C. Cezar, T. Charlton, R. Dalgliesh, C. Bernhard, G. Cristiani, H.-U. Habermeier, B. Keimer, Magnetism at the interface between ferromagnetic and superconducting oxides, *Nat. Phys.* 2 (2006) 244–248.
- [10] J. Chakhalian, J.W. Freeland, H.-U. Habermeier, G. Cristiani, G. Khaliullin, M. van Veenendaal, B. Keimer, Orbital reconstruction and covalent bonding at an oxide interface, *Science* 318 (2007) 1114–1117.
- [11] J. Hoppler, J. Stahn, C. Niedermayer, V.K. Malik, H. Bouyanfif, A.J. Drew, M. Rossle, A. Buzdin, G. Cristiani, H.-U. Habermeier, B. Keimer, C. Bernhard, Giant superconductivity-induced modulation of the ferromagnetic magnetization in a cuprate–manganite superlattice, *Nat. Mater.* 8 (2009) 315–319.
- [12] K. Ueno, S. Nakamura, H. Shimotani, A. Ohtomo, N. Kimura, T. Nojima, H. Aoki, Y. Iwasa, M. Kawasaki, Electric-field-induced superconductivity in an insulator, *Nat. Mater.* 7 (2008) 855–858.
- [13] K.S. Takahashi, M. Gabay, D. Jaccard, K. Shibuya, T. Ohnishi, M. Lippmaa, J.-M. Triscone, Local switching of two-dimensional superconductivity using the ferroelectric field effect, *Nature* 441 (2006) 195–198.
- [14] C.H. Ahn, J.-M. Triscone, J. Mannhart, Electric field effect in correlated oxide systems, *Nature* 424 (2003) 1015–1018.
- [15] C.H. Ahn, A. Bhattacharya, M. Di Ventra, J.N. Eckstein, C.D. Frisbie, M.E. Gershenson, A.M. Goldman, I.H. Inoue, J. Mannhart, A.J. Millis, A.F. Morpurgo, D. Natelson, J.-M. Triscone, Electrostatic modification of novel materials, *Rev. Modern Phys.* 78 (2006) 1185.
- [16] S. Kivelson, Making high  $T_c$  higher: A theoretical proposal, *J. Phys. B: Condens. Matter* 318 (2002) 61–67.
- [17] E. Berg, D. Orgad, S. Kivelson, Route to high-temperature superconductivity in composite systems, *Phys. Rev. B* 78 (2008) 094509.
- [18] O. Yuli, I. Asulin, O. Millo, D. Orgad, L. Iomin, G. Koren, Enhancement of the superconducting transition temperature of  $\text{La}_{2-x}\text{Sr}_x\text{CuO}_4$  bilayers: Role of pairing and phase stiffness, *Phys. Rev. Lett.* 101 (2008) 057005.
- [19] V. Berezinskii, *Zh. Eksper. Teoret. Fiz.* 61 (1971) 1144.
- [20] V.L. Berezinskii, Destruction of long-range order in one-dimensional and two-dimensional systems possessing a continuous symmetry group. II. Quantum systems, *Sov. Phys. JETP* 34 (1971) 610.
- [21] J.M. Kosterlitz, D.J. Thouless, Long range order and metastability in two dimensional solids and superfluids. (Application of dislocation theory), *J. Phys. C* 5 (1972) L124.
- [22] A. Gozar, G. Logvenov, L.F. Kourkoutis, A.T. Bollinger, L.A. Giannuzzi, D.A. Muller, I. Bozovic, High-temperature interface superconductivity between metallic and insulating copper oxides, *Nature* 455 (2008) 782–785.
- [23] G. Logvenov, V. Butko, C. DevilleCavellin, J. Seo, A. Gozar, I. Bozovic, Engineering interfaces in cuprate superconductors, *Phys. B: Condens. Matter* 403 (2008) 1149–1150.
- [24] S. Okamoto, T. Maier, Enhanced superconductivity in superlattices of high- $T_c$  cuprates, *Phys. Rev. Lett.* 101 (2008) 156401.
- [25] S. Smadici, J.C.T. Lee, S. Wang, P. Abbamonte, G. Logvenov, A. Gozar, C.D. Cavellin, I. Bozovic, Superconducting transition at 38 K in insulating-overdoped  $\text{La}_2\text{CuO}_4\text{-La}_{1.64}\text{Sr}_{0.36}\text{CuO}_4$  superlattices: Evidence for interface electronic redistribution from resonant soft X-ray scattering, *Phys. Rev. Lett.* 102 (2009) 107004.
- [26] A. Ohtomo, D.A. Muller, J.L. Grazul, H.Y. Hwang, Artificial charge-modulation in atomic-scale perovskite titanate superlattices, *Nature* 419 (2002) 378–380.
- [27] S. Gariglio, M. Gabay, J.-M. Triscone, Oxide materials: Superconductivity on the other side, *Nat. Nano.* 5 (2010) 13–14.
- [28] G. Logvenov, A. Gozar, I. Bozovic, High-temperature superconductivity in a single copper-oxygen plane, *Science* 326 (2009) 699–702.
- [29] A. Ohtomo, H.Y. Hwang, A high-mobility electron gas at the  $\text{LaAlO}_3/\text{SrTiO}_3$  heterointerface, *Nature* 427 (2004) 423–426.
- [30] S. Gariglio, N. Reyren, A.D. Caviglia, J.-M. Triscone, Superconductivity at the  $\text{LaAlO}_3/\text{SrTiO}_3$  interface, *J. Phys.: Condens. Matter* 21 (2009) 164213.
- [31] N. Nakagawa, H.Y. Hwang, D.A. Muller, Why some interfaces cannot be sharp, *Nat. Mater.* 5 (2006) 204–209.
- [32] R. Pentcheva, W.E. Pickett, Avoiding the polarization catastrophe in  $\text{LaAlO}_3$  overlayers on  $\text{SrTiO}_3(001)$  through polar distortion, *Phys. Rev. Lett.* 102 (2009) 107602.
- [33] J. Lee, A.A. Demkov, Charge origin and localization at the n-type  $\text{SrTiO}_3/\text{LaAlO}_3$  interface, *Phys. Rev. B* 78 (2008) 193104.



- [34] Z.S. Popovic, S. Satpathy, R.M. Martin, Origin of the two-dimensional electron gas carrier density at the  $\text{LaAlO}_3$  on  $\text{SrTiO}_3$  interface, *Phys. Rev. Lett.* 101 (2008) 256801.
- [35] C. Cancellieri, N. Reyren, S. Gariglio, a.D. Caviglia, a. Fête, J.-M. Triscone, Influence of the growth conditions on the  $\text{LaAlO}_3/\text{SrTiO}_3$  interface electronic properties, *Europhys. Lett.* 91 (2010) 17004, and references therein.
- [36] P.R. Willmott, S.A. Pauli, R. Herger, C.M. Schlepütz, D. Martocchia, B.D. Patterson, B. Delley, R. Clarke, D. Kumah, C. Cionca, Y. Yacoby, Structural basis for the conducting interface between  $\text{LaAlO}_3$  and  $\text{SrTiO}_3$ , *Phys. Rev. Lett.* 99 (2007) 155502.
- [37] C.L. Jia, S.B. Mi, M. Faley, U. Poppe, J. Schubert, K. Urban, Oxygen octahedron reconstruction in the  $\text{SrTiO}_3/\text{LaAlO}_3$  heterointerfaces investigated using aberration-corrected ultrahigh-resolution transmission electron microscopy, *Phys. Rev. B* 79 (2009) 081405.
- [38] S. Thiel, G. Hammerl, A. Schmehl, C.W. Schneider, J. Mannhart, Tunable quasi-two-dimensional electron gases in oxide heterostructures, *Science* 313 (2006) 1942–1945.
- [39] N. Reyren, S. Thiel, A.D. Caviglia, L.F. Kourkoutis, G. Hammerl, C. Richter, C.W. Schneider, T. Kopp, A.-S. Ruetschi, D. Jaccard, M. Gabay, D.A. Muller, J.-M. Triscone, J. Mannhart, Superconducting interfaces between insulating oxides, *Science* 317 (2007) 1196–1199.
- [40] N. Reyren, S. Gariglio, a.D. Caviglia, D. Jaccard, T. Schneider, J.-M. Triscone, Anisotropy of the superconducting transport properties of the  $\text{LaAlO}_3/\text{SrTiO}_3$  interface, *Appl. Phys. Lett.* 94 (2009) 112506.
- [41] T. Schneider, a. Caviglia, S. Gariglio, N. Reyren, J.-M. Triscone, Electrostatically-tuned superconductor-metal-insulator quantum transition at the  $\text{LaAlO}_3/\text{SrTiO}_3$  interface, *Phys. Rev. B* 79 (2009) 184502.
- [42] M. Gabay, A. Kapitulnik, Vortex-antivortex crystallization in thin superconducting and superfluid films, *Phys. Rev. Lett.* 71 (1993) 2138.
- [43] L. Benfatto, C. Castellani, T. Giamarchi, Broadening of the Berezinskii–Kosterlitz–Thouless superconducting transition by inhomogeneity and finite-size effects, *Phys. Rev. B* 80 (2009) 214506.
- [44] K. Medvedyeva, B.J. Kim, P. Minnhagen, Analysis of current-voltage characteristics of two-dimensional superconductors: Finite-size scaling behavior in the vicinity of the Kosterlitz–Thouless transition, *Phys. Rev. B* 62 (2000) 14531–14540.
- [45] A.D. Caviglia, S. Gariglio, N. Reyren, D. Jaccard, T. Schneider, M. Gabay, S. Thiel, G. Hammerl, J. Mannhart, J.-M. Triscone, Electric field control of the  $\text{LaAlO}_3/\text{SrTiO}_3$  interface ground state, *Nature* 456 (2008) 624–627.
- [46] D. Matthey, S. Gariglio, J.-M. Triscone, Field-effect experiments in  $\text{NdBa}_2\text{Cu}_3\text{O}_{7.8}$  ultrathin films using a  $\text{SrTiO}_3$  single-crystal gate insulator, *Appl. Phys. Lett.* 83 (2003) 3758.
- [47] G. Bergmann, Weak localization in thin films: A time-of-flight experiment with conduction electrons, *Phys. Rep.* 107 (1984) 1–58.
- [48] C. Bell, S. Harashima, Y. Kozuka, M. Kim, B.G. Kim, Y. Hikita, H.Y. Hwang, Dominant mobility modulation by the electric field effect at the  $\text{LaAlO}_3/\text{SrTiO}_3$  interface, *Phys. Rev. Lett.* 103 (2009) 226802.
- [49] S. Sachdev, *Quantum Phases Transitions*, Cambridge Univ. Press, 1999.
- [50] A.F. Hebard, M.A. Paalanen, Magnetic-field-tuned superconductor–insulator transition in two-dimensional films, *Phys. Rev. Lett.* 65 (1990) 927–930.
- [51] A. Yazdani, W.R. White, M.R. Hahn, M. Gabay, M.R. Beasley, A. Kapitulnik, Observation of Kosterlitz–Thouless-type melting of the disordered vortex lattice in thin films of  $\alpha$ - $\text{MoGe}$ , *Phys. Rev. Lett.* 70 (1993) 505–508.
- [52] A. Yazdani, A. Kapitulnik, Superconducting–insulating transition in two-dimensional  $\alpha$ - $\text{MoGe}$  thin films, *Phys. Rev. Lett.* 74 (1995) 3037–3040.
- [53] C. Cen, S. Thiel, G. Hammerl, C.W. Schneider, K.E. Andersen, C.S. Hellberg, J. Mannhart, J. Levy, Nanoscale control of an interfacial metal–insulator transition at room temperature, *Nat. Mater.* 7 (2008) 298–302.
- [54] A.D. Caviglia, S. Gariglio, C. Cancellieri, B. Sacepe, A. Fête, N. Reyren, M. Gabay, A.F. Morpurgo, J.-M. Triscone, Two-dimensional quantum oscillations of the conductance at  $\text{LaAlO}_3/\text{SrTiO}_3$  interfaces, *Phys. Rev. Lett.* 105 (2010) 236802.